Community Radiative Transfer Model (CRTM) for NOAA Remote Sensing Data cal/val and Products

Quanhua (Mark) Liu[1], Ming Chen[2,3], Kevin J. Garrett[1,3], Changyong Cao[1], and Benjamin Johnson[3]

1. NOAA/NESDIS Center for Satellite Applications and Research, College Park, Maryland, USA
2. University of Maryland, College Park, Maryland, USA
3. Joint Center for Satellite Data Assimilation, College Park, Maryland, USA

2019 International Workshop on Radiative Transfer Models for Satellite Data Assimilation, Tianjin, April 29 – May 03, 2019

Outlines

- CRTM – A radiance interpreter for applications
- CRTM support Sensor data Cal/Val
  1) CrIS O - B
  2) VIIRS O – B
  3) VIIRS M12 striping investigation
  4) CrIS Spectral Assessment
- Microwave Integrated Retrieval System (MiRS)
- Vectorized CRTM
- AI based Radiative Transfer Calculations
- Discussion

What is Community Radiative Transfer Model (CRTM)? --- Radiance interpreter

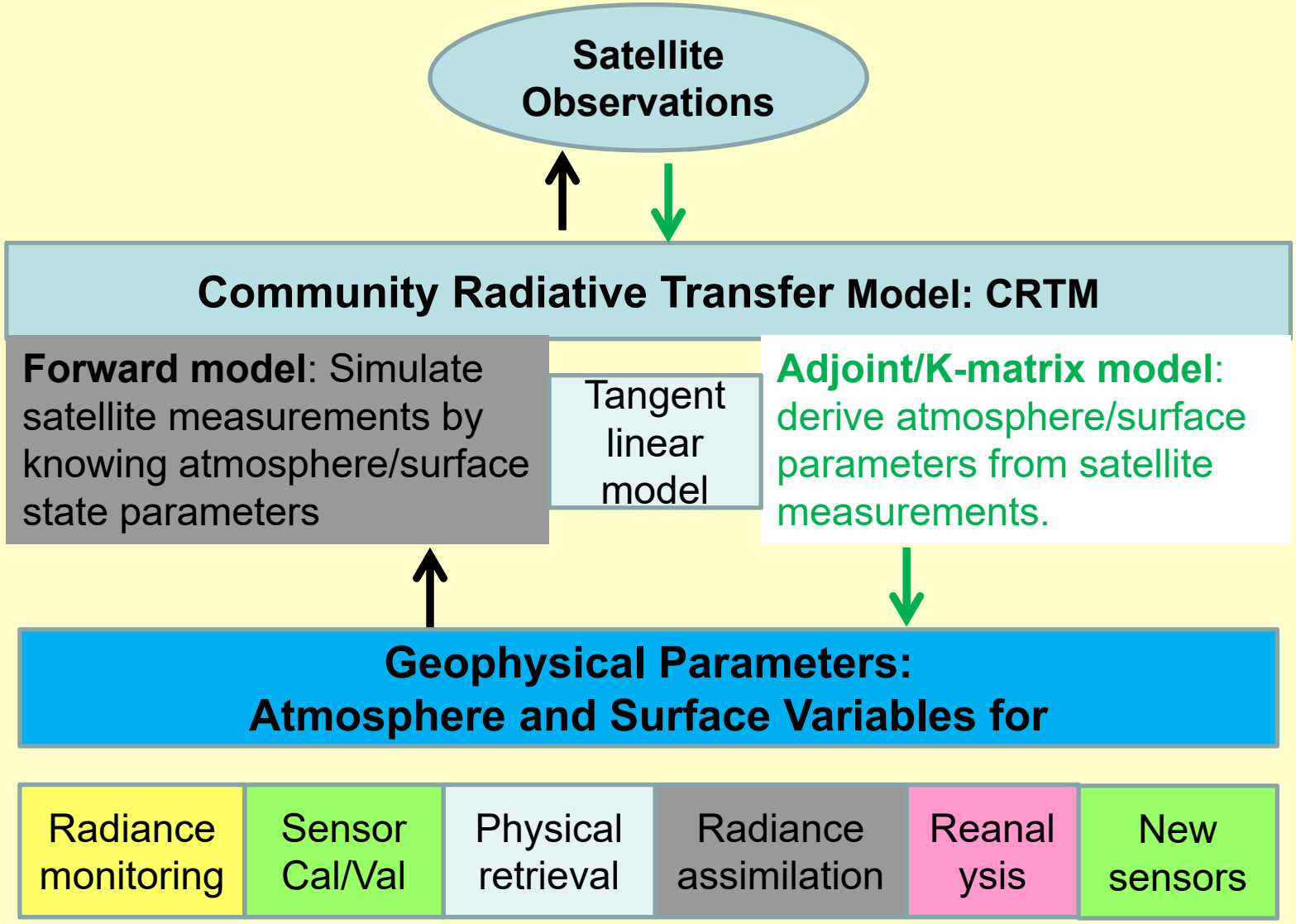

NOAA/NESDIS STAR ICVS
NOAA-20 CrIS Observations - Simulations

CrIS observation (O) – CRTM simulations (B) using ECMWF model data

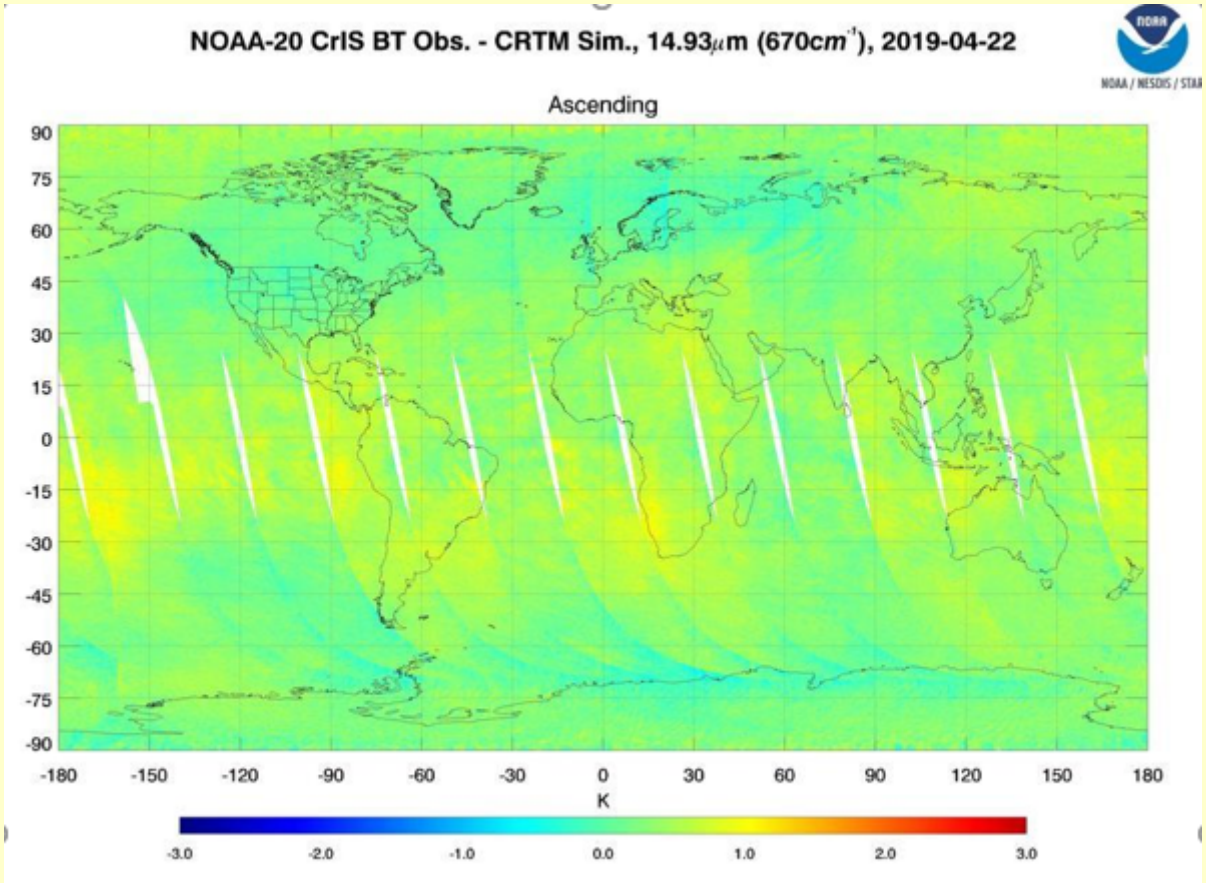

NOAA/NESDIS STAR ICVS
NOAA-20 VIIRS (O – B)

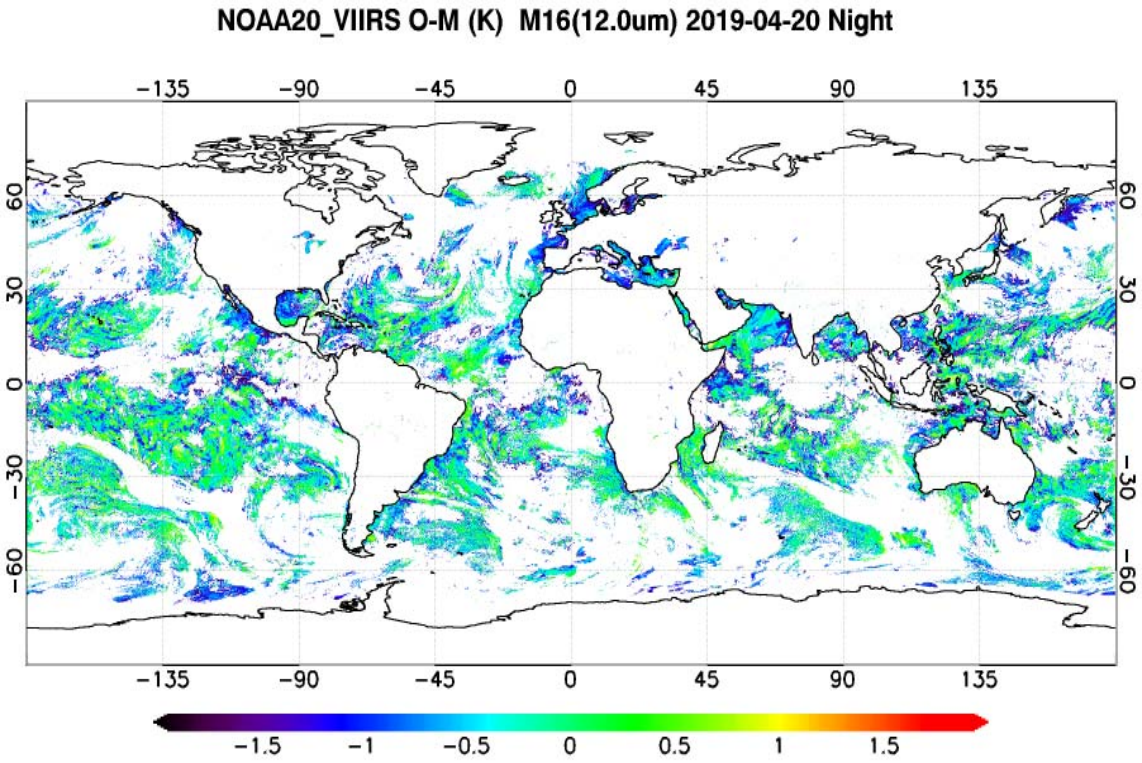

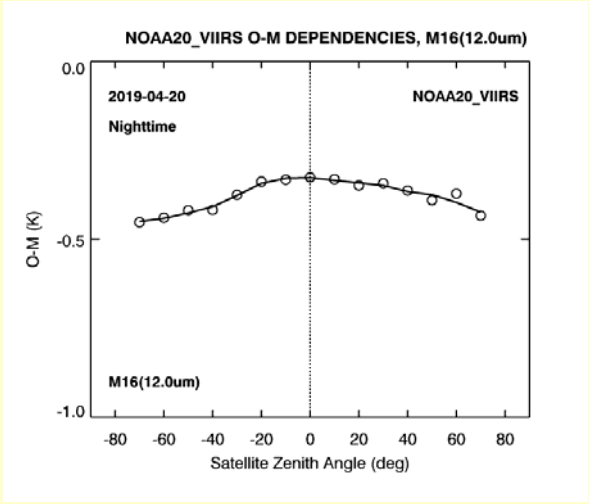

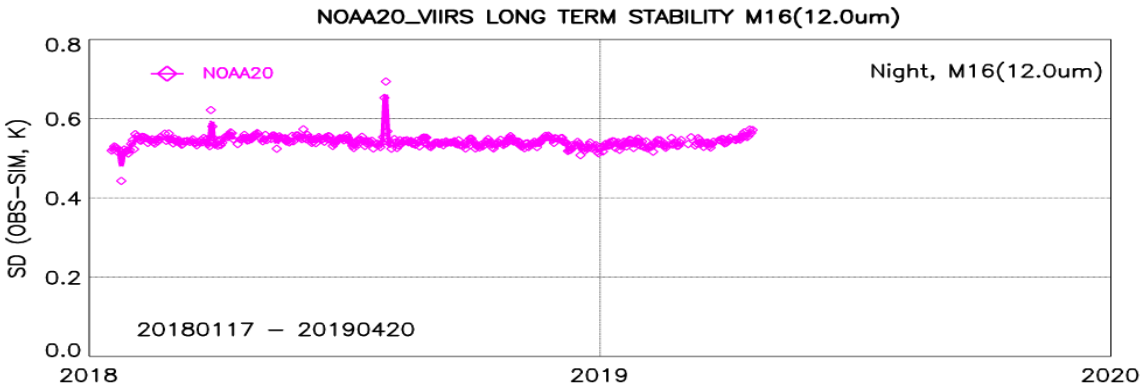

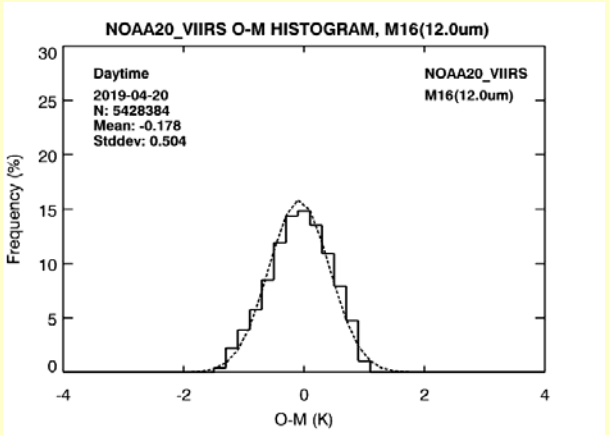

CrIS Spectral Assessment: Cross-Correlation Method

Two basic spectral validation methods are used to assess the CrIS SDR spectral accuracy

Relative spectral validation, which uses two uniform observations to determine frequency offsets relative to each other

Absolute spectral validation, which requires an accurate forward model to simulate the top of atmosphere radiance under clear conditions and correlates the simulation with the observed radiance to find the maximum correlation

Correlation coefficient between the two spectra:

$$r_{S_1S_2} = \frac{\sum_{i=1}^{n}(S_{1,i}-\overline{S_1})(S_{2,i}-\overline{S_2})}{(n-1)D_{S_1}D_{S_2}} = \frac{\sum_{i=1}^{n}(S_{1,i}-\overline{S_1})(S_{2,i}-\overline{S_2})}{\sqrt{\sum_{i=1}^{n}(S_{1,i}-\overline{S_1})^2(S_{2,i}-\overline{S_2})^2}}$$

Standard deviation based on the difference of the two spectra:

$$D_{S_1S_2} = \sqrt{\sum_{i=1}^{n}[(S_{1,i}-\overline{S_1})-(S_{2,i}-\overline{S_2})]^2} \Big/ (n-1)$$

The cross-correlation method is applied to a pair fine grid spectra to get the maximum correlation and minimum standard deviation by shifting one of the spectra in a given shift factor

CrIS Spectral Uncertainty

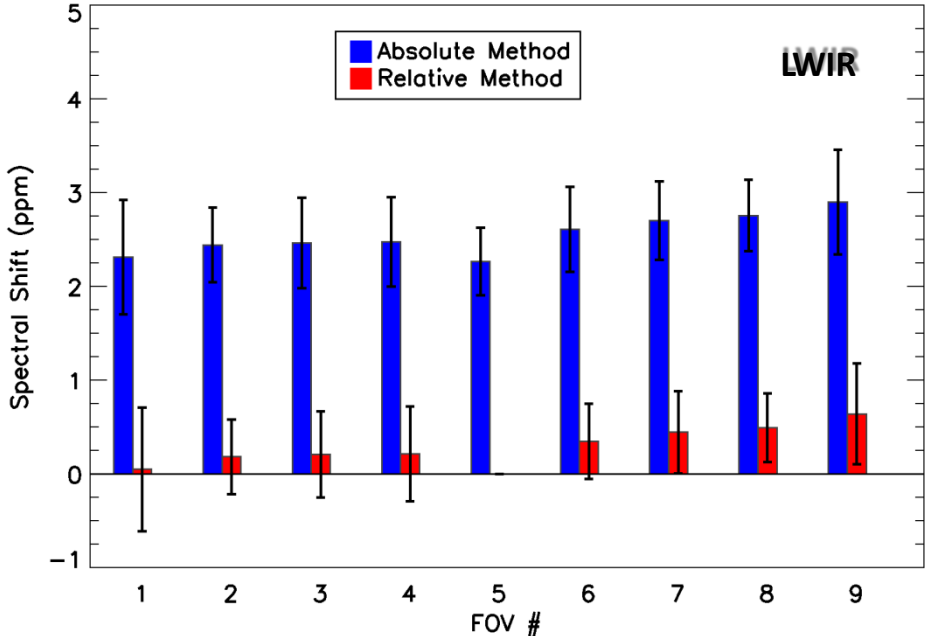

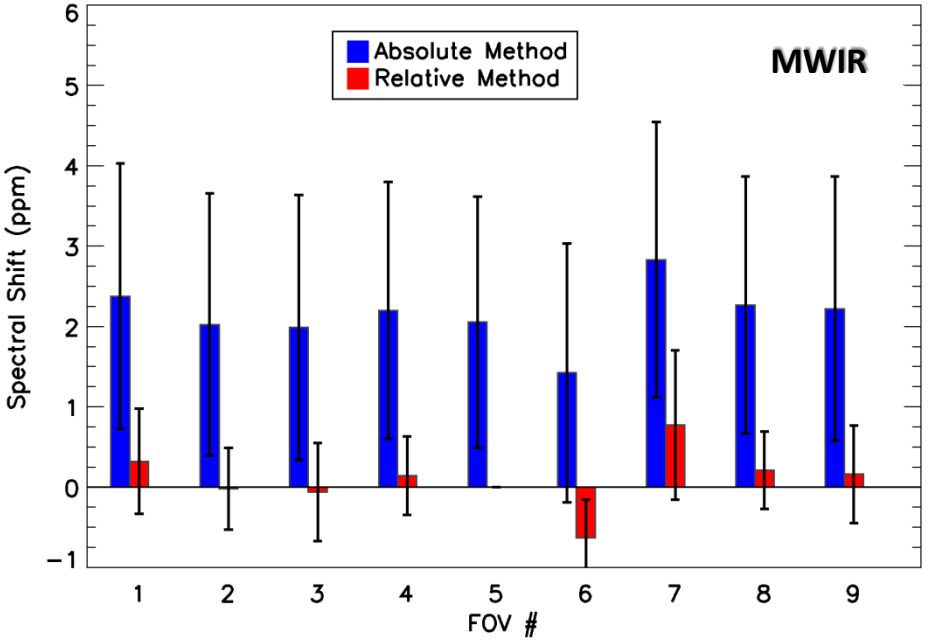

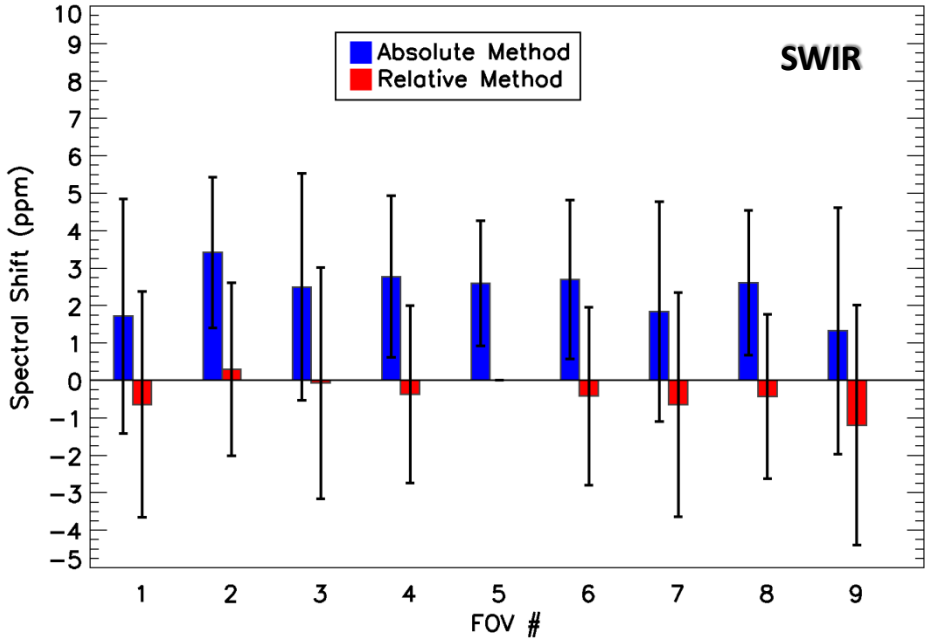

- Absolute cross-correlation method: between observations and CRTM simulations under clear sky over oceans to detect the spectral shift
- Relative method: observations from FOV 5 to other FOVs
- Frequency used: 710-760 cm^{-1} , 1340-1390 cm^{-1} , and 2310-2370 cm^{-1}
- **Spectral shift relative to FOV5 are within 1 ppm**
- **Absolute spectral shift relative to CRTM within 3 ppm.**

VIIRS and CRTM Modeling for M12 Striping Investigation

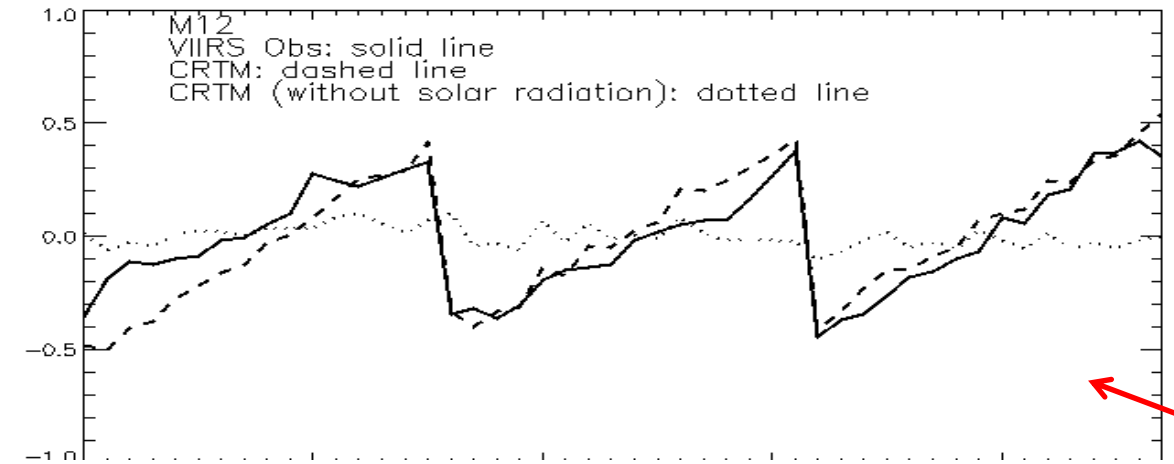

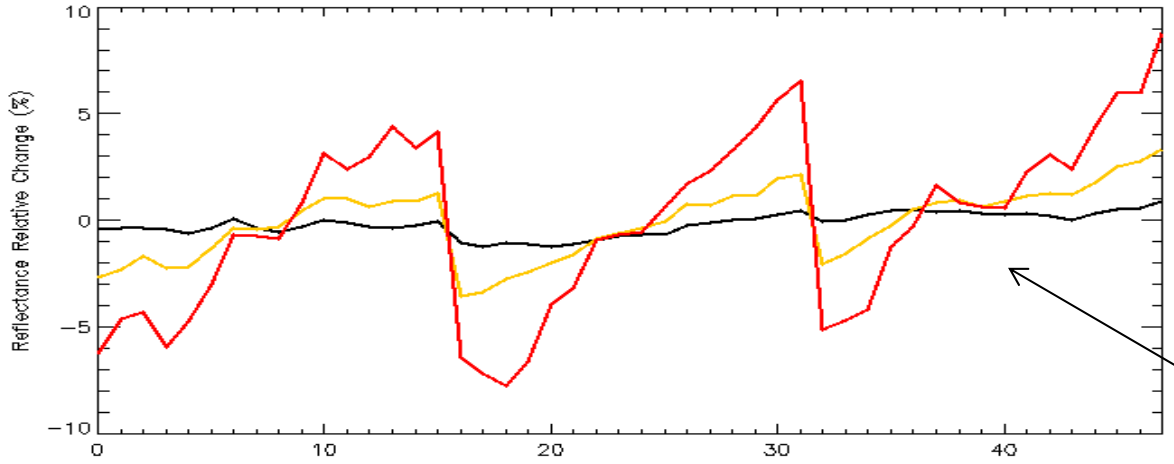

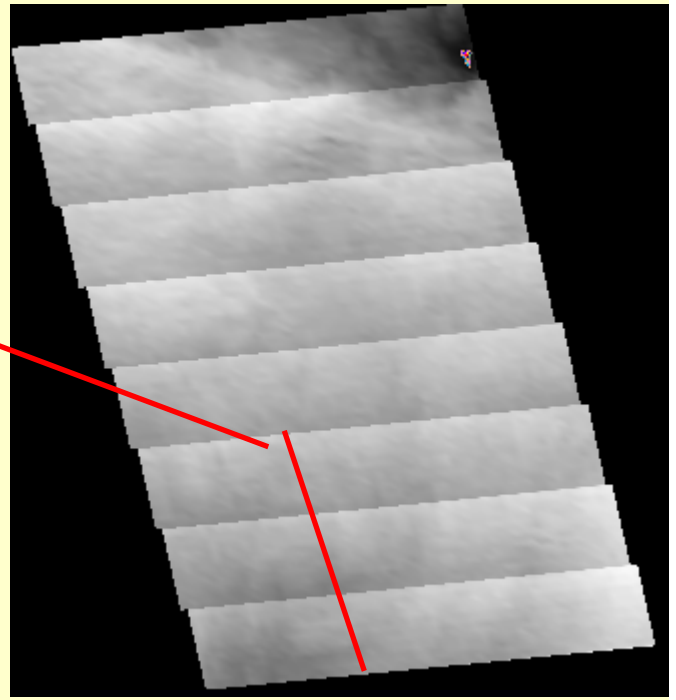

M1, M4, and M11 measured (R-Rm)/Rm *100

The STAR team applied the CRTM to simulate the VIIRS SDR data.
It is found that the M12 striping reported by the SST EDR team is caused by the difference in VIIRS azimuth angles among detectors.

Detailed CRTM Calculation for the Striping

Detector #	$\tau(\theta_{sat})$	ϕ_{sat}	BRDF	**A**	**B**	R	Brightness temperature
1	0.73685	80.368	0.04253	0.51055	0.10590	0.61645	302.666
2	0.73649	80.543	0.04309	0.50923	0.10717	0.61641	302.648
3	0.73700	80.717	0.04365	0.51022	0.10873	0.61894	302.738
4	0.73645	80.892	0.04422	0.50964	0.10999	0.61962	302.769
5	0.73705	81.066	0.04479	0.51114	0.11159	0.62273	302.871
6	0.73628	81.241	0.04537	0.51147	0.11280	0.62427	302.931
7	0.73701	81.415	0.04596	0.51164	0.11448	0.62612	302.987
8	0.73596	81.589	0.04656	0.51074	0.11566	0.62640	303.020
9	0.73673	81.764	0.04715	0.51175	0.11739	0.62914	303.115
10	0.73557	81.938	0.04776	0.51124	0.11855	0.62978	303.153
11	0.73641	82.113	0.04837	0.51120	0.12036	0.63157	303.230
12	0.73509	82.287	0.04901	0.51134	0.12155	0.63289	303.316
13	0.73562	82.461	0.04962	0.51180	0.12325	0.63505	303.396
14	0.73486	82.636	0.05026	0.51057	0.12461	0.63518	303.417
15	0.73526	82.810	0.05089	0.50993	0.12629	0.63622	303.439
16	0.73565	82.985	0.05154	0.50998	0.12812	0.63810	303.560

$$R = \tau(\theta_{sat})[\varepsilon B(T_s) + (1-\varepsilon)R_{atm\_d}] + R_{atm\_u} + F_0 \cos(\theta_{sun})\tau(\theta_{sun})BRDF(\theta_{sun}, \theta_{sat}, \phi_{sun} - \phi_{sat})\tau(\theta_{sat})$$

A B

NOAA Microwave Integrated Retrieval System Algorithm Background

MiRS: Microwave Integrated Retrieval System

Run on Satellites:
- SNPP/ATMS
- N18
- N19
- Metop-A
- Metop-B
- F17
- F18
- GPM/GMI
- Megha-Torpiques/SAPIR
- NOAA-20/ATMS
- Metop-C
- JPSS-2 (Next)
- ….

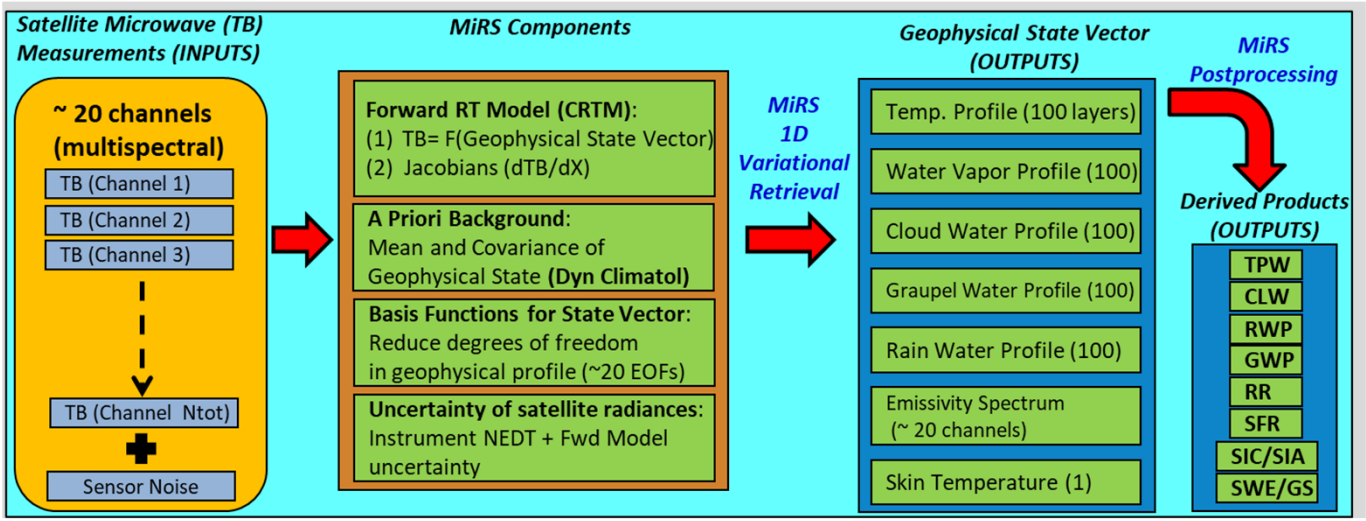

Variational approach: find the "most likely" atmosphere/surface state that
- Best matches satellite measurements
- is still close to an a priori estimate of atmosphere/surface conditions

MiRS one-dimensional variation

- Cost Function to minimize:

$$J(X)=\left[\frac{1}{2}\underbrace{(X-X_0)^T\times B^{-1}\times(X-X_0)}\right]+\left[\frac{1}{2}\underbrace{(Y^m-Y(X))^T\times E^{-1}\times(Y^m-Y(X))}\right]$$

Bkg-departure normalized by Bkg Error

Measurements-departure normalized by Measurements+Modeling Errors

Previously updated in V11

- To find the optimal solution, solve for: $\frac{\partial J(X)}{\partial X}=J'(X)=0$

- Assuming local Linearity: $y(x)=y(x_0)+K\left[x-x_0\right]$

- This leads to iterative solution:

$$\Delta X_{n+1}=\left\{BK_n^T\left(K_nBK_n^T+E\right)^{-1}\right\}\left[\left(Y^m-Y(X_n)\right)+K_n\Delta X_n\right]$$

Validation Results: Temperature Profile

Global all Condition T Statistic refer to ECMWF

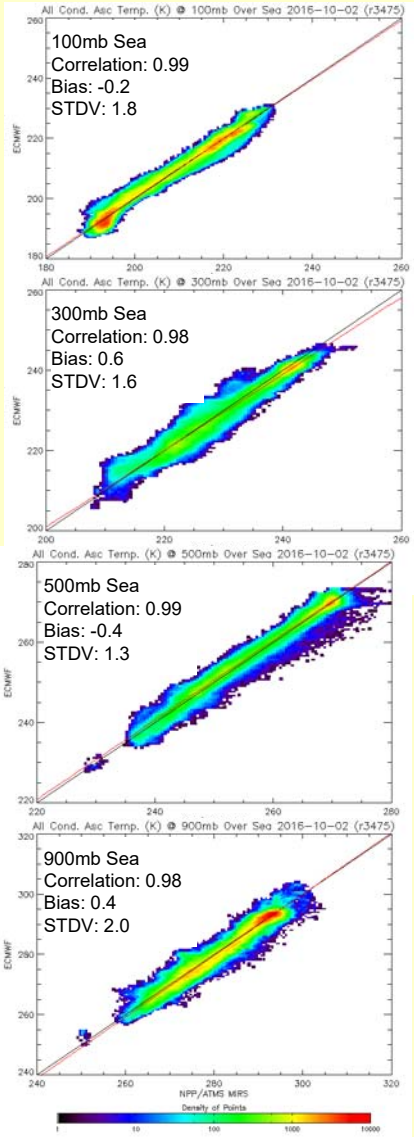

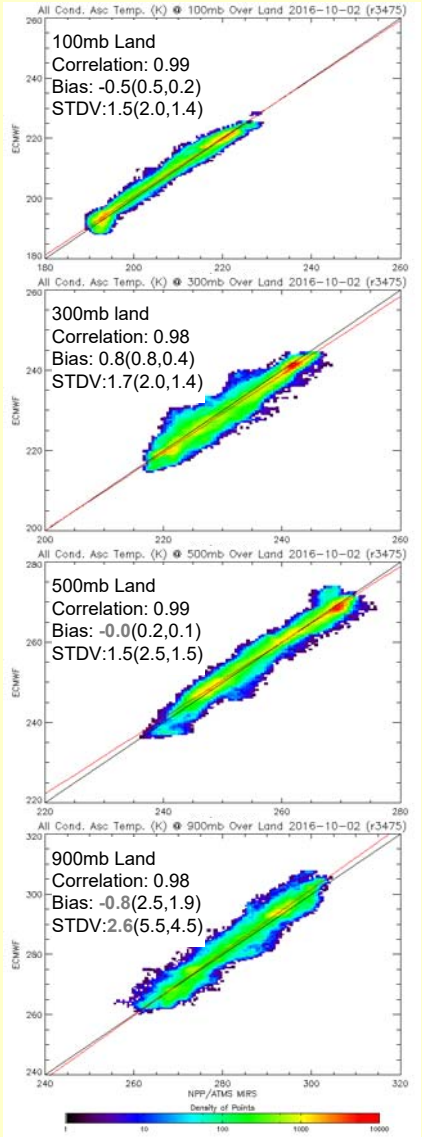

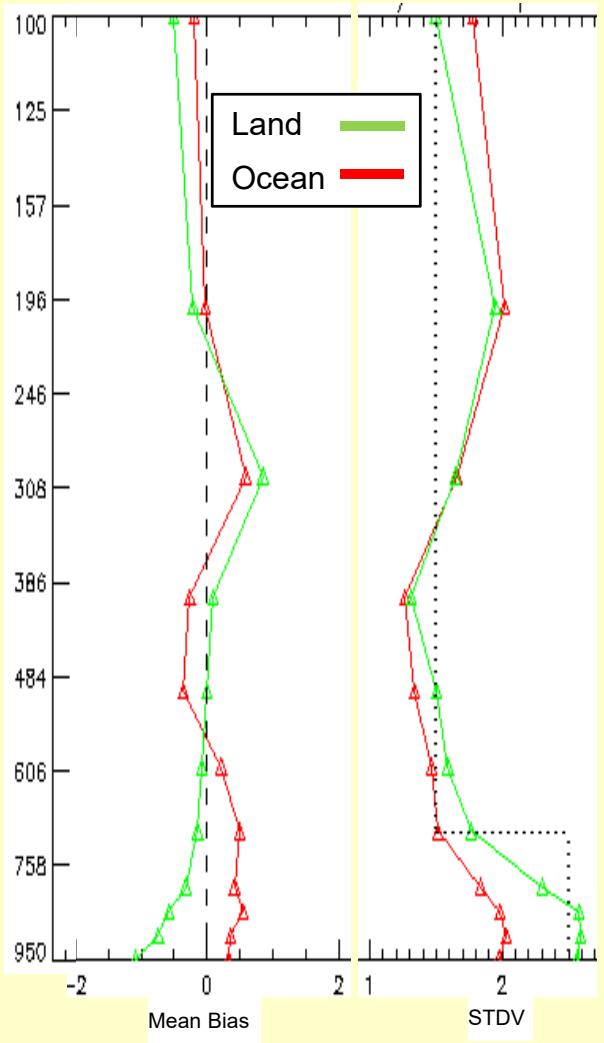

Radiances in studying Hurricane (warm core from SSMIS observations at 54.4 GHz)

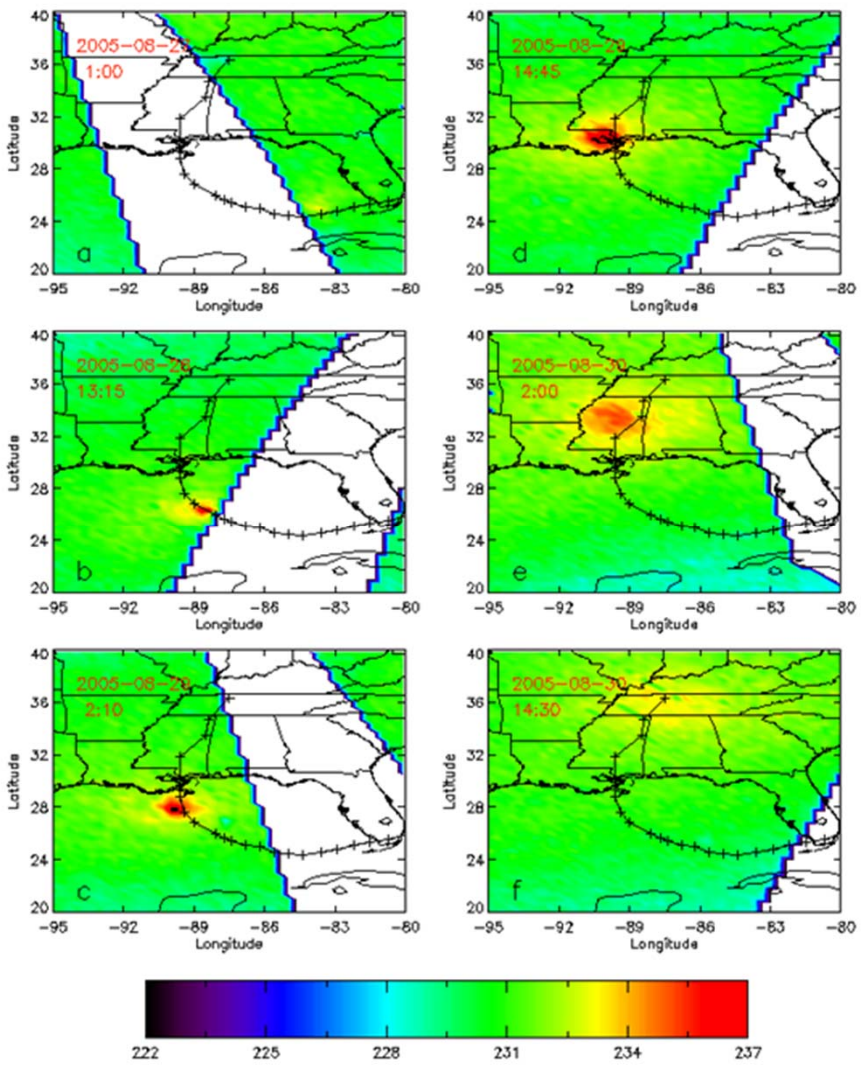

The SSMIS (F16) measures radiances in 24 channels covering a wide range of frequencies (19 – 183 GHz) conical scan geometry at an earth incidence angle of 53 degrees maintains uniform spatial resolution, across the entire swath of 1700 km.

The images left showed warm core (~200 hPa) of hurricane Katrina in 2005. It got strengthen over Ocean and weakened after landfall.

Comparison between test-run and control-run
Only a case study

Forecasting time (hour)	Surface minimum pressure (hPa)			Surface maximum wind (m/s)		
	Control	Test	Observation	Control	Test	Observation
00	988.87	983.31	959.00	26.18	31.51	46.20
06	981.55	974.60	950.00	36.36	30.46	48.80
12	970.80	957.90	942.00	39.05	39.33	51.40
18	964.45	945.81	948.00	39.97	48.99	51.40
24	951.71	936.11	941.00	45.19	49.31	51.40
30	935.58	923.40	930.00	49.40	57.20	64.20
36	927.75	913.17	909.00	54.86	58.20	74.50
42	918.92	908.72	902.00	57.94	58.31	77.10
48	916.38	905.25	905.00	54.31	59.67	71.90

Validation Results: Rain Rate

NOAA-20

January 2018

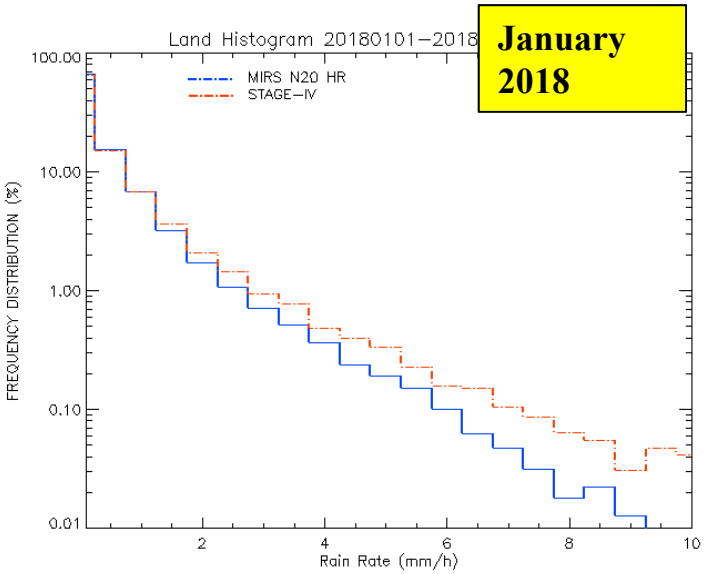

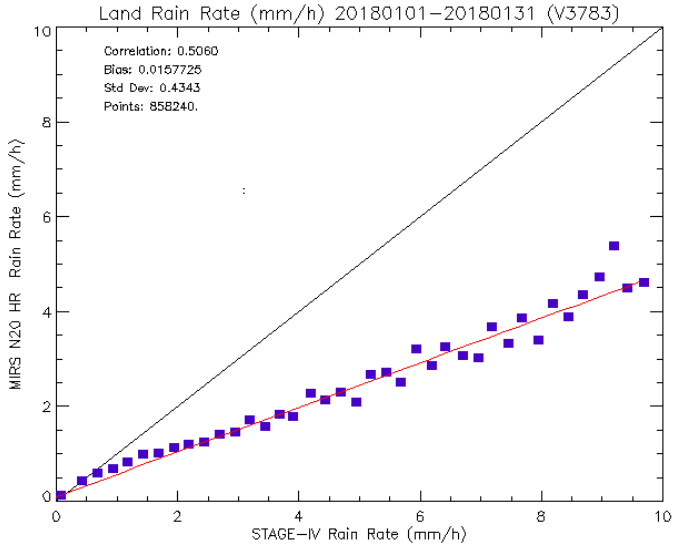

July 2018

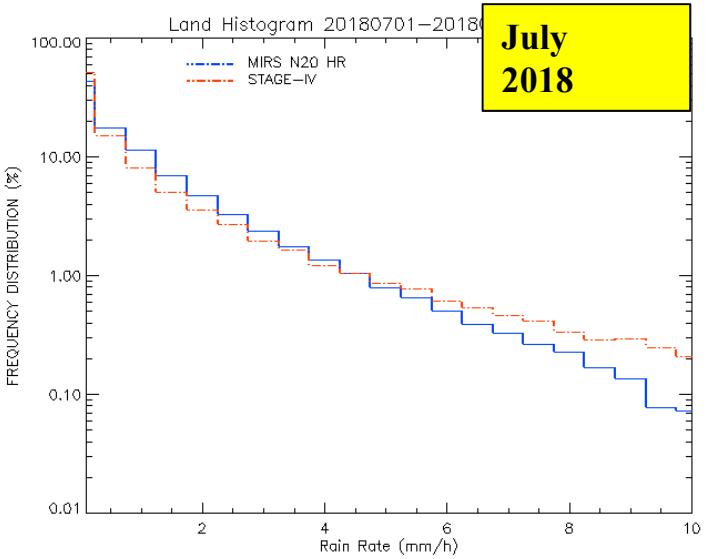

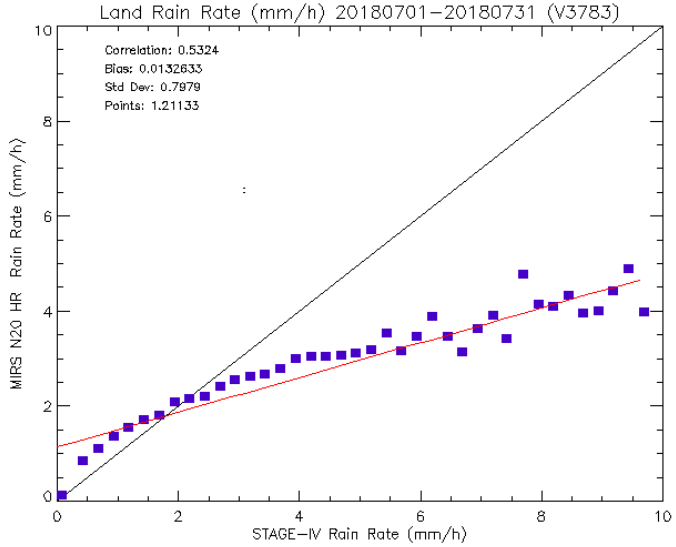

Vectorized CRTM

We initially investigate 3 options for vectorized CRTM:

1. Extend ADA (mainly enlarge array size from n_stream to n_stokes x n_stream), very little code change, but slow
2. Extend AMOM, lots of code change because of complex eigensolution
3. Extend ADA for > base optical depth, a new subroutine (~50 line code) for <= base optical depth, a compromise code change and efficiency

We chose option 3, since the algorithm is simple for TL and AD coding. FWD, TL, and AD are completed and tested.

The vectorized CRTM TL/AD is for radiances (VIS/UV). For BT (IR, MW), some code change needs to be done.

Option 2 will be investigated later.

Radiative Transfer Solver (AMOM)

Layer transmittance (t) and reflection (r) matrices and source vector (s)

$$\boldsymbol{t} = 2[\cosh(\boldsymbol{H}\delta) - \boldsymbol{V}\sinh(\boldsymbol{H}\delta) + \cosh(\boldsymbol{F}\delta) - \boldsymbol{U}\sinh(\boldsymbol{F}\delta)]^{-1} \quad (8c)$$

and the layer reflection matrix is,

$$\boldsymbol{r} = \frac{1}{2}[\cosh(\boldsymbol{H}\delta) + \boldsymbol{V}\sinh(\boldsymbol{H}\delta) - \cosh(\boldsymbol{F}\delta) - \boldsymbol{U}\sinh(\boldsymbol{F}\delta)]\boldsymbol{t} \quad (8d)$$

$$\boldsymbol{s}_u = \left[(\boldsymbol{E} - \boldsymbol{t} - \boldsymbol{r})B(T_1) - (B(T_2) - B(T_1))\boldsymbol{t} + \frac{B(T_2) - B(T_1)}{(1 - \varpi g)\delta}(\boldsymbol{E} + \boldsymbol{r} - \boldsymbol{t})\boldsymbol{u}\right]\Xi\delta_{0m} + e^{-\frac{\tau_0}{\mu_0}}\left[\left(\boldsymbol{E} - \boldsymbol{t}e^{-\frac{\delta}{\mu_0}}\right)\boldsymbol{\Psi}_u - \boldsymbol{r}\boldsymbol{\Psi}_d\right]$$

$$\boldsymbol{s}_d = \left[(\boldsymbol{E} - \boldsymbol{t} - \boldsymbol{r})B(T_1) + (B(T_2) - B(T_1))(\boldsymbol{E} - \boldsymbol{r}) + \frac{B(T_2) - B(T_1)}{(1 - \varpi g)\delta}(\boldsymbol{t} - \boldsymbol{E} - \boldsymbol{r})\boldsymbol{u}\right]\Xi\delta_{0m} + e^{-\frac{\tau_0}{\mu_0}}\left[\left(e^{-\frac{\delta}{\mu_0}}\boldsymbol{E} - \boldsymbol{t}\right)\boldsymbol{\Psi}_d - \boldsymbol{r}e^{-\frac{\delta}{\mu_0}}\boldsymbol{\Psi}_u\right]$$

Integrated layers and surface (k=0 for TOP and k=n_Layers for surface)

$$\boldsymbol{R}_u(k-1) = \boldsymbol{r}(k) + \boldsymbol{t}(k)[\boldsymbol{E} - \boldsymbol{R}_u(k)\boldsymbol{r}(k)]^{-1}\boldsymbol{R}_u(k)\boldsymbol{t}(k) \quad (9a)$$

$$\boldsymbol{I}_u(k-1) = \boldsymbol{s}_u(k) + \boldsymbol{t}(k)[\boldsymbol{E} - \boldsymbol{R}_u(k)\boldsymbol{r}(k)]^{-1}[\boldsymbol{R}_u(k)\boldsymbol{s}_d(k) + \boldsymbol{I}_u(k)] \quad (9b)$$

$$\boldsymbol{I}_u = \boldsymbol{I}_u(0) + \boldsymbol{R}_u(0)\boldsymbol{I}_{sky}$$

Vectorized Radiative Transfer Solver

Expansion of array size from n_Angles to n_Stokes x n_Angles, then we can use advanced doubling algorithm (ADA) and TL/AD coding easy, but slow ($\Delta = \delta_0 \times 2^n$, $\delta_0 = 10^{-8}$).

Using AMOM, we have to solve complex Eigensolution, require a big effort in TL, AD coding.

We use a quick solution:

the reciprocity principle in radiative transfer and applies a Taylor expansion of analytic transmittance and reflection matrices for a base optical depth together with a doubling-adding method beyond the base in

$$\cosh(\boldsymbol{H}\delta) - \boldsymbol{V}\sinh(\boldsymbol{H}\delta) + \cosh(\boldsymbol{F}\delta) - \boldsymbol{U}\sinh(\boldsymbol{F}\delta)$$
$$= \sum_0^N \frac{\left[(\alpha-\beta)(\alpha+\beta)\right]^n + \left[(\alpha+\beta)(\alpha-\beta)\right]^n}{(2n)!}\delta^{2n}$$
$$- \sum_0^N \frac{(\alpha+\beta)\left[(\alpha-\beta)(\alpha+\beta)\right]^n + (\alpha-\beta)\left[(\alpha+\beta)(\alpha-\beta)\right]^n}{(2n+1)!}\delta^{2n+1}$$

$$\cosh(\boldsymbol{H}\delta) + \boldsymbol{V}\sinh(\boldsymbol{H}\delta) - \cosh(\boldsymbol{F}\delta) - \boldsymbol{U}\sinh(\boldsymbol{F}\delta)$$
$$= \sum_0^N \frac{\left[(\alpha-\beta)(\alpha+\beta)\right]^n - \left[(\alpha+\beta)(\alpha-\beta)\right]^n}{(2n)!}\delta^{2n}$$
$$+ \sum_0^N \frac{(\alpha+\beta)\left[(\alpha-\beta)(\alpha+\beta)\right]^n + (\alpha-\beta)\left[(\alpha+\beta)(\alpha-\beta)\right]^n}{(2n+1)!}\delta^{2n+1}$$

Two-type expansion of the phase matrix

Table 2a
Legendre expansion coefficients for an atmosphere of randomly oriented oblate spheroids.

	F_{11}	F_{22}	F_{33}	F_{44}	F_{12}	F_{43}
0	1.0	0.0	0.929287	0.0	0.967924	0.915207
1	2.104031	0.0	2.118711	0.0	2.073916	2.095727
2	2.095158	−0.116688	3.615946	0.065456	3.726079	2.008624
3	1.414939	−0.209370	2.240516	0.221658	2.208680	1.436545
4	0.703593	−0.227137	1.139473	0.097752	1.190694	0.706244
5	0.235001	−0.144524	0.365605	0.052458	0.391203	0.238475
6	0.064039	−0.052640	0.082779	0.009239	0.105556	0.056448
7	0.012837	−0.012400	0.013649	0.001411	0.020484	0.009703
8	0.002010	−0.002093	0.001721	0.000133	0.003097	0.001267
9	0.000246	−0.000267	0.000172	0.000011	0.000366	0.000130
10	0.000024	−0.000027	0.000014	0.000001	0.000035	0.000011
11	0.000002	−0.000002	0.000001	0.0	0.000003	0.000001

Table 2b
Greek matrix coefficients for an atmosphere of randomly oriented oblate spheroids.

	F_{11}	F_{22}	F_{33}	F_{44}	F_{12}	F_{43}
0	1.0	0.0	0.0	0.915267	0.0	0.0
1	2.104031	0.0	0.0	0.095727	0.0	0.0
2	2.095158	3.726079	3.615946	2.008624	−0.116688	0.065456
3	1.414939	2.202868	2.240516	1.436545	−0.209370	0.221658
4	0.703593	1.190694	1.139473	0.706244	−0.227137	0.097752
5	0.235001	0.391203	0.365605	0.238475	−0.144524	0.052458
6	0.064039	0.105556	0.082779	0.056448	−0.052640	0.009239
7	0.012837	0.020484	0.013649	0.009703	−0.012400	0.001411
8	0.002010	0.003097	0.001721	0.001267	−0.002093	0.000133
9	0.000246	0.000366	0.000172	0.000130	−0.000267	0.000011
10	0.000024	0.000035	0.000014	0.000011	−0.000027	0.000001
11	0.000002	0.000003	0.000001	0.000001	−0.000002	0.0

Cross comparisons among RT models

Table 7
Same as Table 6, but for an optical depth of 1.

	I	Q	U	V
DA	0.247890	0.001246	−0.007078	0.000019
VLIDORT	0.247882	0.001246	−0.007078	0.000019
ADA	0.247888	0.001246	−0.007077	0.000019
AMOM	0.247888	0.001246	−0.007077	0.000019

Table 8
Same as Table 6, but for an optical depth of 10.

	I	Q	U	V
DA	0.557838	0.003928	−0.012050	0.000044
VLIDORT	0.557727	0.003927	−0.012050	0.000044
ADA	0.557839	0.003928	−0.012050	0.000044
AMOM	0.557828	0.003928	−0.012050	0.000044

Table 10
Comparison of CPU time usage between VLIDORT and AMOM. Phase function for an atmosphere of randomly oriented oblate spheroids and 16 streams are used. The solar flux is normalized to π, the solar zenith angle is 36.8699 (the cosine of the solar zenith angle is 0.8), and the surface albedo is 0.25. Single scattering albedo is 1.0. VLIDORT requires the single scattering is less than 1.0 and we use the single scattering albedo of 0.99999. The upwelling radiance is for a viewing (zenith) angle of 50.21°.

Layer optical depth	VLIDORT (seconds)	AMOM (seconds)
100	0.096	0.076
10	0.096	0.063
1	0.096	0.054
0.1	0.095	0.048

ML-BT Architecture

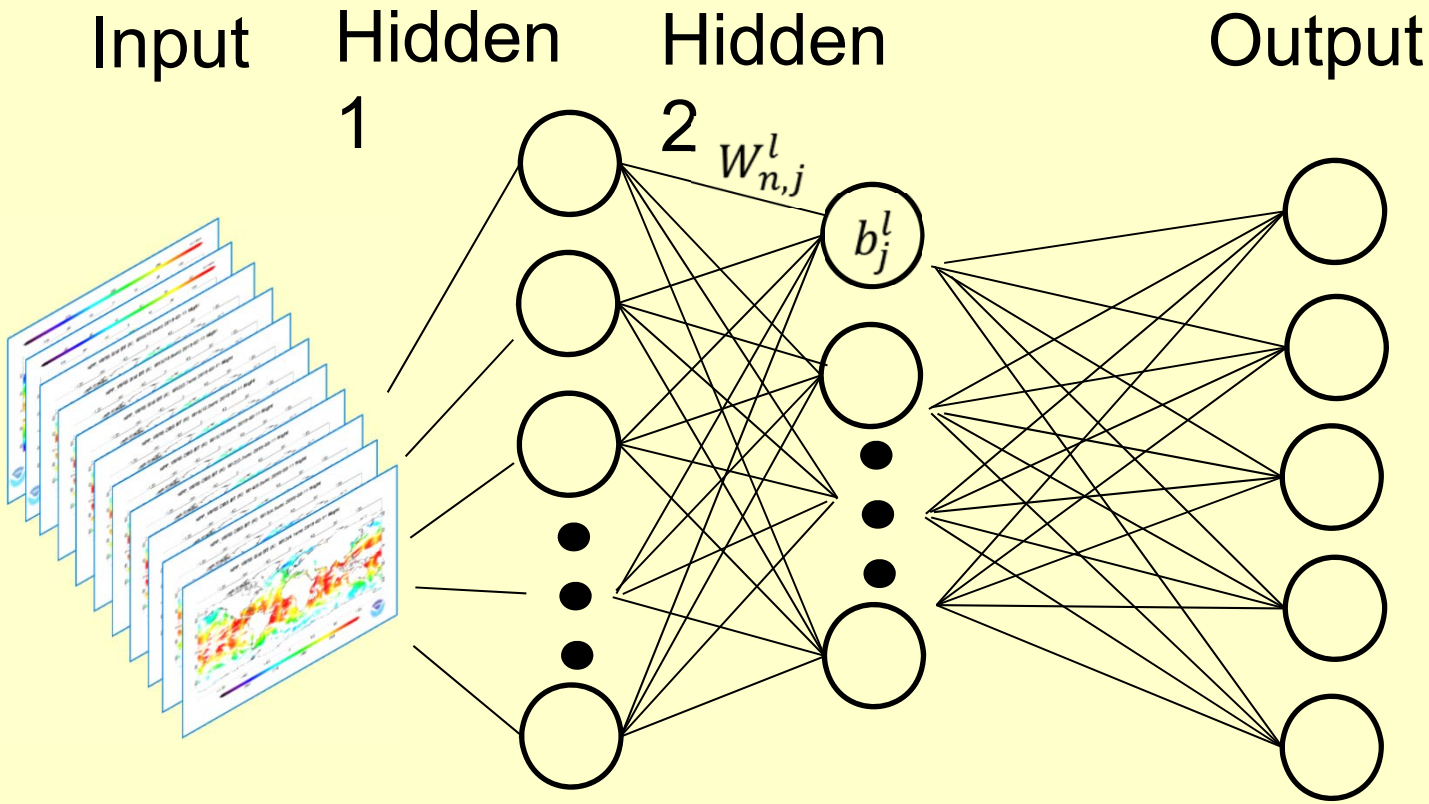

- Fully Connected ANN
- H1: 90 nodes, H2: 40 nodes
- Reference: CRTM BTs

Loss Converges

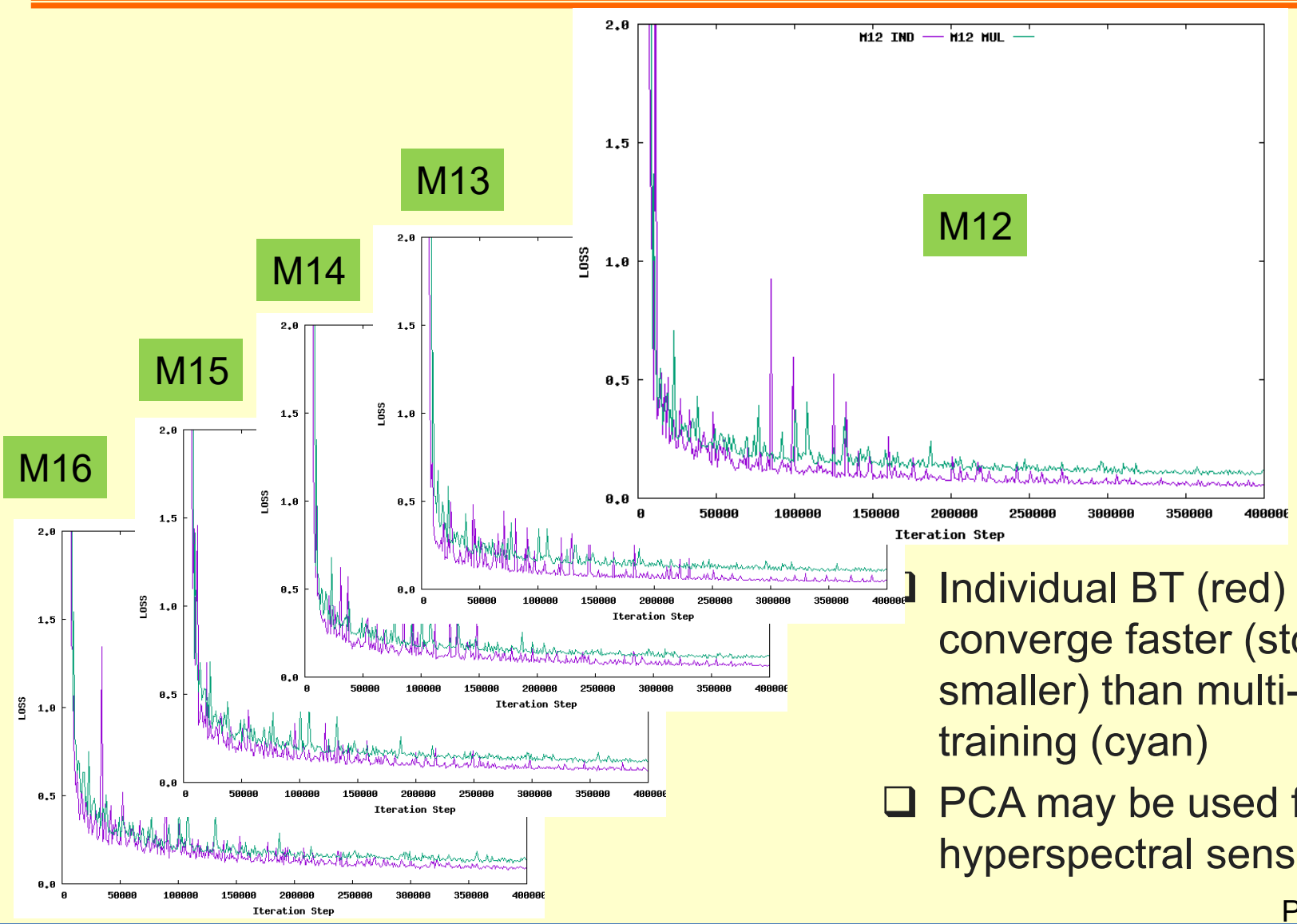

- Individual BT (red) training converge faster (std also smaller) than multi- BT training (cyan)
- PCA may be used for hyperspectral sensors.

Bias and STD (ML-CRTM)

	$\mu_{(IND)}$	$\sigma_{(IND)}$	$\mu_{(MUL)}$	$\sigma_{(MUL)}$	CRTM vs LBLrtm	NOAA-20 VIIRS NEdT
M12	0.0168	0.1108	0.0207	0.1262	0.004	0.12
M13	-0.0052	0.0995	0.0155	0.1681	0.007	0.04
M14	-0.0113	0.1809	0.0195	0.1919	0.015	0.05
M15	-0.0171	0.1593	0.0198	0.1989	0.011	0.02
M16	0.0089	0.1886	0.0107	0.2404	0.013	0.03

- Under clear-sky conditions, AI based RT is harder to achieve CRTM accuracy.
- Single channel AI has better accuracy than multi-channel AI.
- Too many coefficients for single channel AI for hyperspectral sensors. PCA may be an option.
- AI RT may do better job for scattering.
- AI simulation error in channel-2-channel correlation?

Discussions

This presentation demonstrated the CRTM applications:

- Instrument monitoring in ICVS
- ATMS accuracy assessment
- VIIRS striping investigation due to different azimuths among detectors.
- MIRS environmental data

Vectorized CRTM for FWD, TL, AD, and K-Matrix are completed and tested.

AI-based RT for clear-sky cases is demonstrated (should be improved) and will be tested for scattering cases.